ISSN 0031-918X, The Physics of Metals and Metallography, 2015, Vol. 116, No. 1, pp. 97–108. © Pleiades Publishing, Ltd., 2015.
Original Russian Text © A.V. Dobromyslov, N.I. Taluts, E.A. Kozlov, A.V. Petrovtsev, A.T. Sapozhnikov, D.T. Yusupov, 2015, published in Fizika Metallov i Metallovedenie, 2015, Vol. 116, No. 1, pp. 101–113.

STRENGTH AND PLASTICITY

Deformation Behavior of Copper under Conditions of Loading by Spherically Converging Shock Waves: High-Intensity Regime of Loading

A. V. Dobromyslov[a], N. I. Taluts[a], E. A. Kozlov[b], A. V. Petrovtsev[b], A. T. Sapozhnikov[b], and D. T. Yusupov[b]

[a] *Institute of Metal Physics, Ural Branch, Russian Academy of Sciences, ul. S. Kovalevskoi 18, Ekaterinburg, 620990 Russia*

[b] *Russian Federal Nuclear Center, Zababakhin All-Russia Research Institute of Technical Physics, a/ya 245, Snezhinsk, Chelyabinsk oblast, 456770 Russia*

e-mail: Dobromyslov@imp.uran.ru

Received June 21, 2013; in final form May 26, 2014

Abstract—Methods of X-ray diffraction analysis, optical metallography, transmission electron microscopy, and microhardness measurements have been used to perform a layer-by-layer study of the structure of a 64-mm copper ball after loading by spherically converging shock waves. It has been revealed that the high-velocity plastic deformation of copper under these loading conditions is mainly realized via slip and, in the middle and deep layers, by the formation of localized-deformation bands at grain boundaries. On the macroscopic level, shear bands are observed and, on the microlevel, a homogeneous dislocation structure, microbands, microtwins, a banded structure, and dislocation vacancy loops arise.

Keywords: shock waves, high-velocity plastic deformation, copper, structure

DOI: 10.1134/S0031918X15010044

INTRODUCTION

The effects of shock waves on the structure and strain hardening of copper have been studied for 50 years. It follows from the results obtained that after shock-wave loading copper exhibits a significant variety of deformation structures [1–13]. This is due to the fact that the occurrence of high-velocity plastic deformation of copper is affected by many parameters of both the initial structure and the shock impact. The mechanism of the high-velocity plastic deformation depends on whether the sample is single-crystal or polycrystalline; in the case of a polycrystalline sample, it also depends on the grain size. On the other hand, this mechanism is strongly affected by the magnitude of the pressure at the front of the shock wave, duration of the shock pulse, shape of the pulse, direction of the propagation of the shock wave in the single crystal, and the loading mode. To date, most experiments were performed using retained samples loaded by plane shock waves.

In our previous work [13], we have studied the structure and mechanisms of high-velocity plastic deformation of polycrystalline coarse-grained copper after explosive loading of a 70-mm ball by spherically converging shock isentropic waves. It has been established that under the loading conditions employed the main mechanism of plastic deformation of polycrystalline copper is slip, while twinning plays only a secondary role. In the process of high-velocity plastic deformation, there are formed shear bands that mainly belong to one and the same slip system. On the microlevel, the deformation structure is characterized by a homogeneous distribution of dislocations (without the formation of a cellular structure) and by the presence of microbands and a small amount of microtwins.

This work is a continuation of the work [13] and is devoted to the study of the deformation structure and mechanisms of high-velocity plastic deformation of polycrystalline copper at a stronger shock loading of a 64-mm ball by spherically converging shock isentropic waves, which made it possible to increase the energy introduced into the sample by a factor of approximately 1.5.

EXPERIMENTAL

Polycrystalline copper of grade M1 was used as the material for the investigation. A ball-shaped sample 64 mm in diameter was obtained from a copper rod 80 mm in diameter. The loading was performed by a quasi-spherical converging detonation wave initiated in a layer of a power explosive based on hexogen (RDX-based composition) with an external radius $R_{expl} = 40$ mm and a thickness of 8 mm (Fig. 1a). The flying of the explosion products in this experiment was

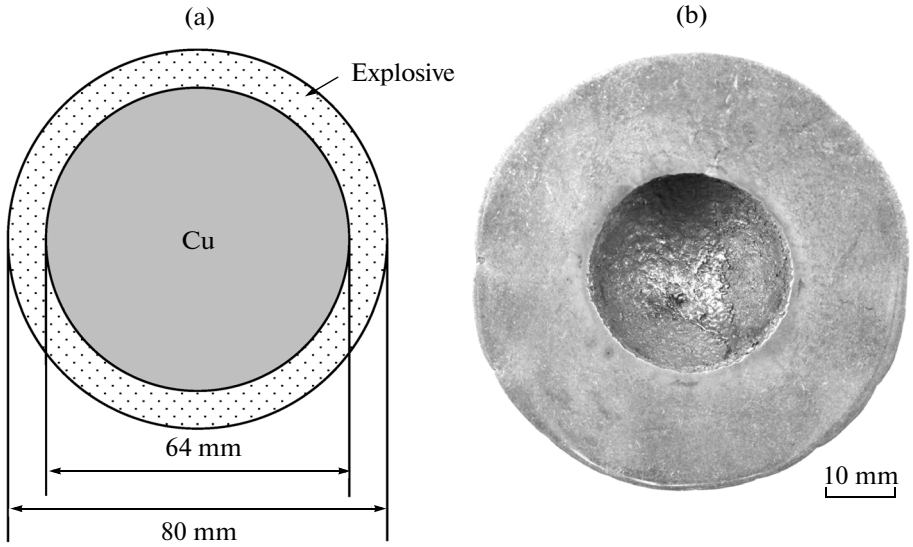

Fig. 1. (a) Scheme of loading and (b) the appearance of a meridional section of the ball of polycrystalline copper after explosive loading.

restricted by a heavy casing made of cast iron. The residual thermal energy of the sample that remained unbroken after the spherical explosion compression was 100 kJ. The retained shock-loaded sample was cut along the meridional section. To analyze the evolution of the structure and to measure microhardness, the section was polished (Fig. 1b). For the investigation, X-ray diffraction, optical microscopy, transmission electron microscopy, and measurements of microhardness along the radial direction were used. For the layer-by-layer analysis, a rod of a square section was cut out from the ball along one of the radial directions. This rod was cut perpendicular to the radial direction to prepare metallographic polished sections and thin foils at different distances from the external surface of the ball.

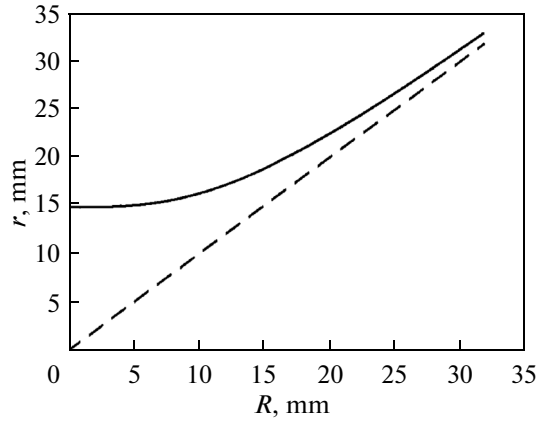

Fig. 2. Change in the location of the layers in the ball after loading.

To study microstructure, a NEOPHOT-32 optical microscope and JEM-200CX and Philips CM 30 electron microscopes were used. The XRD analysis was performed using a DRON-3 diffractometer. The microhardness was measured using a PMT-3 microhardness meter under a load of 0.49 N.

RESULTS

In the process of explosive loading, the initially continuous ball acquired the form of a thick-walled shell with an external radius of ~33 mm and a cavity in the central part (Fig. 1b). The cavity has a shape close to spherical and is located symmetrically with respect to the ball center. On the surface of the cavity, there are present traces of molten copper, and around the cavity a region of crystallized metal exists. The appearance of the cavity surface indicates the occurrence of plastic fracture in the process of its formation. The volume of the internal cavity is $V_c = 14.113$ cm^3, and the average radius of the cavity is $R_c = 14.99$ mm. The formation of the cavity led to displacements of the layers that, in the initial ball, were located in positions R to the positions r (Fig. 2).

To estimate the conditions of the ball loading and variations in pressure over time for a number Lagrangian particles separated in the copper ball, one-dimensional calculations were performed using a wide-range equation of state with allowance for the evaporation of the substance (Fig. 3) [14, 15]. The initial pressure on the surface of the copper ball was ~50 GPa. The amplitude of the loading first decreased somewhat moving away from the ball surface, then remained almost constant in some layer and only increased in deeper layers at $R/R_{expl} \le 0.3$ because of

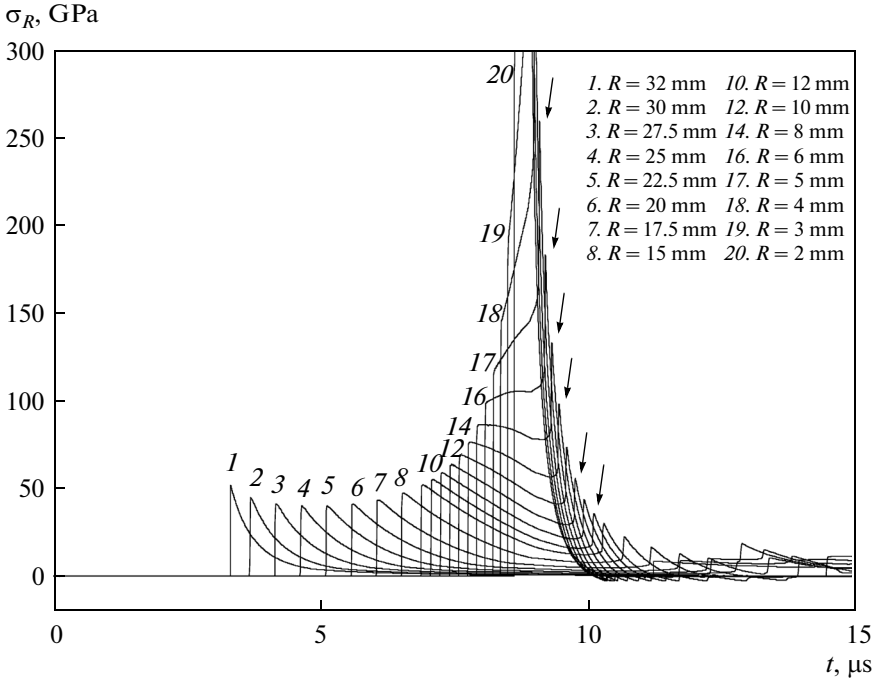

Fig. 3. Calculated estimates of the variations in pressure σ_R over time at the boundary of the copper ball that initially was located at $R = 32$ mm (curve *1*), and the calculated time variations of the radial components of stresses for a number of Lagrangian particles separated in the copper ball that initially were located at the indicated radii (curves *2*–*20*). Arrows indicate the moments at which the shock wave reflected from the center reached the corresponding Lagrangian particle.

the accumulation of energy at the front of the converging wave. At the relative radius $R = 0.1R_{expl}$ (4 mm), the amplitude of the loading in the converging wave was calculated to be 145 GPa. At $0.35 \le R/R_{expl} \le 0.8$, the pressure at the front of the converging shock wave was varied from 40 to 50 GPa.

The X-ray diffraction analysis shows that the X-ray diffraction patterns obtained from the sample in the initial state contain a doublet of $K\alpha_1$ and $K\alpha_2$ lines for all reflections beginning with 022. After explosive loading, the doublet splitting in the X-ray diffraction patterns disappears because of the smearing of diffraction lines for all reflections *hkl*. The half-width of the diffraction lines increases as compared to the half-widths of the lines in the initial state; the greatest broadening is observed in the layers located at radii *r* higher than 21.4 mm (see table). With a further increase in the depth of the layer location, there occurs a decrease in the line half-width related to a temperature increase in these layers, which leads to the development of processes of recovery and recrystallization.

In the initial state, the average grain size is equal to ~300 μm. Many grains contain annealing twins of various shape and size. Along with the annealing twins of a large size, there also observed thin twins ~5–10 μm

Broadening of X-ray diffraction lines of polycrystalline copper ball after loading the ball via spherically converging shock waves at different distances from the external surface of the ball

r, mm	Reflection indices *hkl*				
	002	022	113	133	024
Initial state	0.23°	0.32°	0.39°	0.97°	1.20°
31.4	0.31°	0.41°	0.55°	1.25°	1.75°
28.9	0.31°	0.42°	0.57°	1.27°	1.73°
26.4	0.31°	0.41°	0.58°	1.31°	1.79°
23.9	0.30°	0.40°	0.62°	1.25°	1.82°
21.4	0.31°	0.41°	0.58°	1.24°	1.79°
20.0	0.30°	0.36°	0.53°	1.27°	1.63°
18.9	0.30°	0.37°	0.52°	1.12°	1.63°

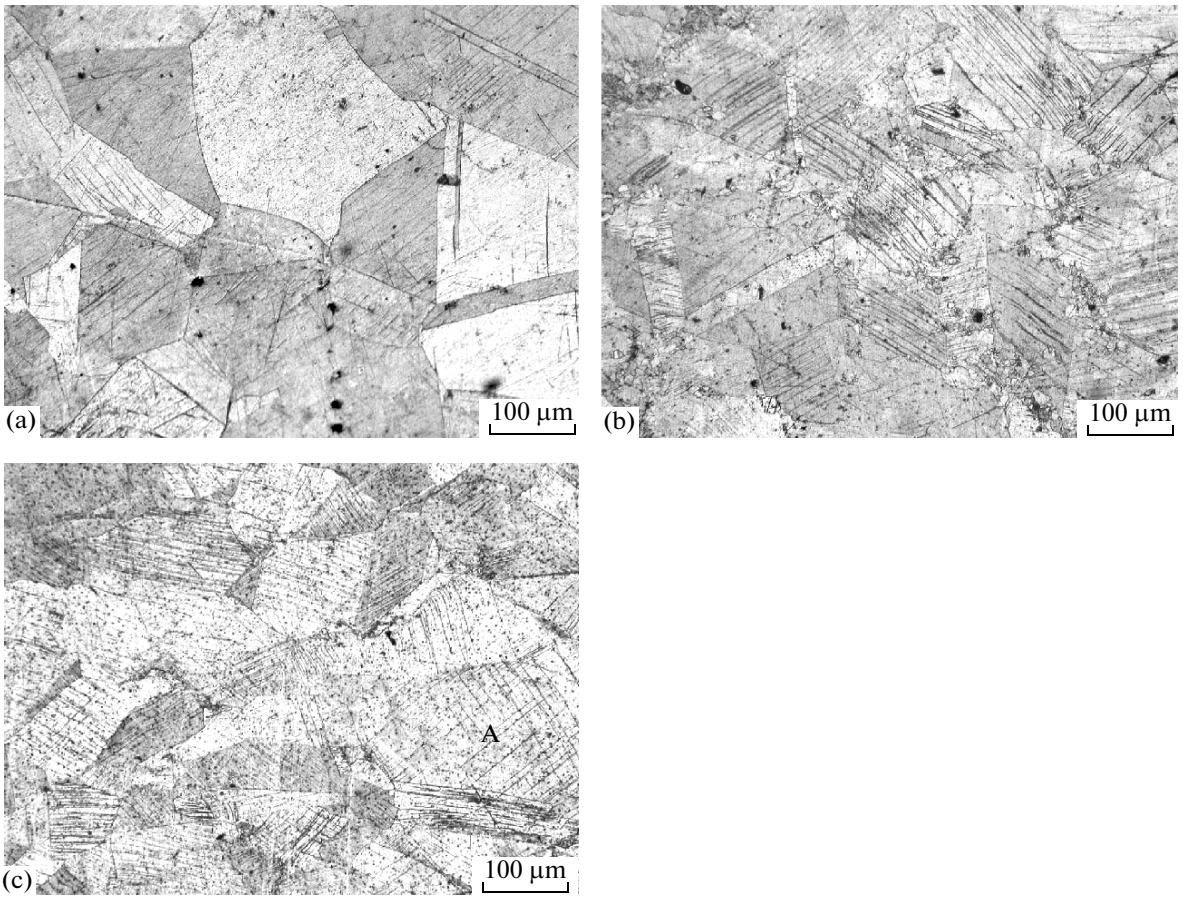

Fig. 4. Structure of copper in different regions (located at radii r) in the retained sample: (a) $r = 31.3$; (b) 30.3; and (c) 25.3 mm.

thick propagating from grain boundaries. After explosive loading, the structure of the subsurface layers changes only a little as compared to the structure of copper in the initial state (Fig. 4a). The grains retain their initial shape; signs of plastic deformation appear only in some grains in the form of slip traces or shear bands. Upon moving from the loading surface by 2.5 mm, the length and the density of shear bands increase (Fig. 4b). The shear bands mainly belong to one slip system, although traces of two slip systems can be revealed in some grains. Along with the shear bands, twins appear to be present in the deformation structure of copper. Metallographically, it is difficult to distinguish them from shear bands since they propagate in the same set of planes {111}. In Fig. 4c, in the region designated as A, two systems of thin lines are observed apart from shear bands; based on their appearance and thickness and the character of the location, they differ substantially from shear bands. These defects appear to be twins.

Overall, this character of the structure is retained up to the layers located at $r = 23.8$ mm; however, beginning with these layers, a change is observed in the appearance of some boundaries at which a large amount of very fine grains is present that are located mainly on grain segments oriented perpendicular to the direction of propagation of the shock wave. With increasing the depth of the layer location, the bands of fine grains located around the initial grains become more extended (Fig. 5a). With further approaching to the cavity, there begins grain refinement, which is related to processes of recrystallization (Fig. 5b). In the layers located near the cavity, the structure consists only of fine recrystallized grains. A layer of columnar crystals is observed around the cavity that is formed upon the solidification of molten copper (Fig. 5c). On average, the thickness of this layer is ~100 μm.

A substantial difference between the deformation structure of copper after high-intensity and low-intensity loading described in [13] is the formation of localized-deformation bands at grain boundaries. These bands can have different thicknesses and lengths (Fig. 6). The nucleation of bands of localized deformation appear to occur at structure defects. No bands of adiabatic shear occurs in this sample, just as in the sample subjected to low-intensity loading.

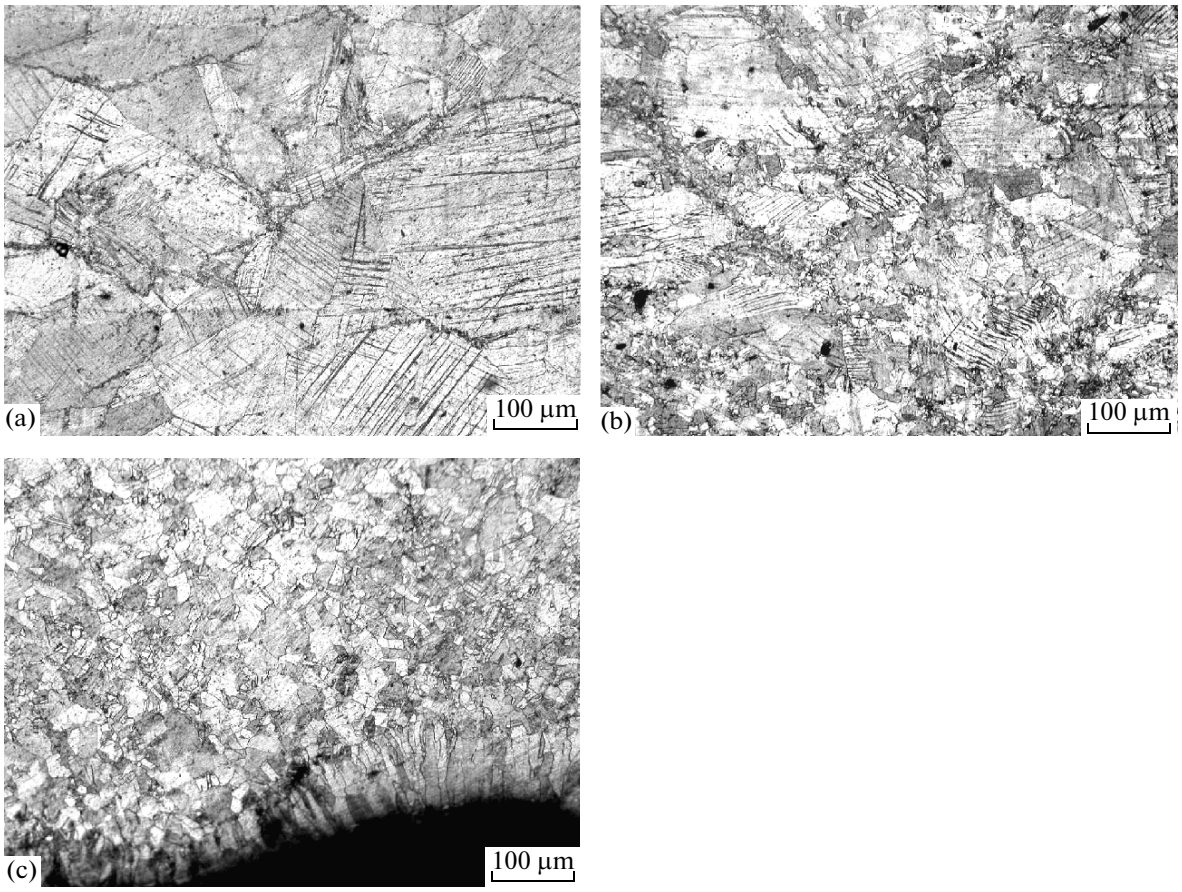

Fig. 5. Structure of copper in different regions (located at radii r) in the retained sample: (a) $r = 22.3$; (b) 19.3; and (c) 15.8 mm.

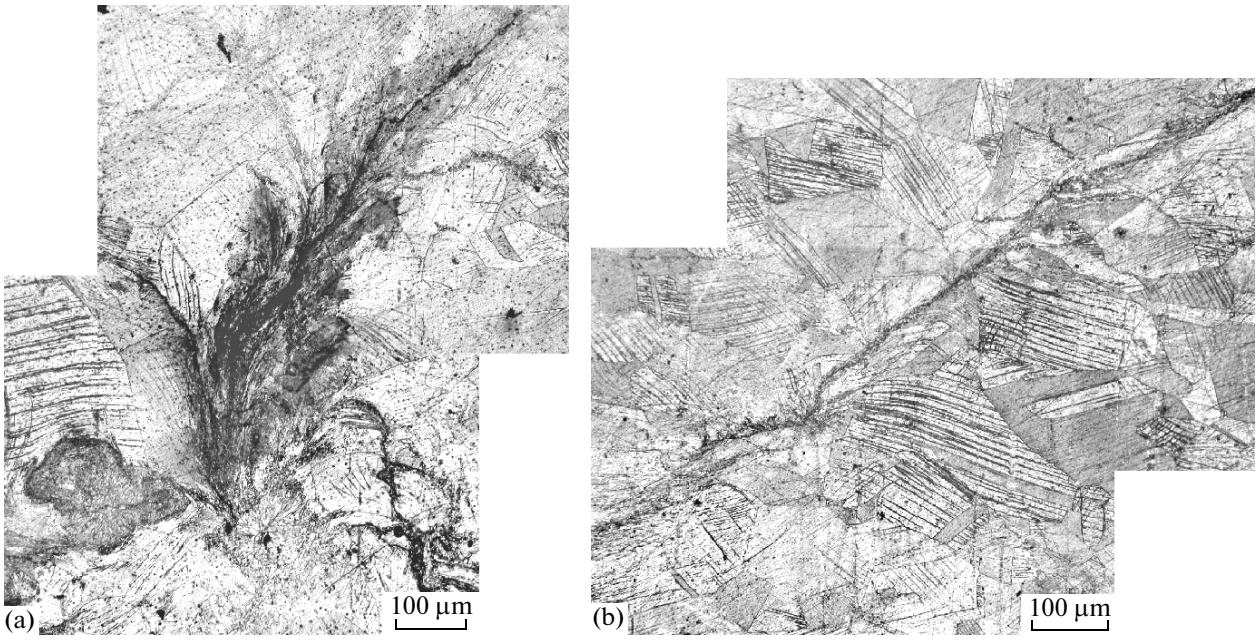

Fig. 6. Localized-deformation bands at grain boundaries.

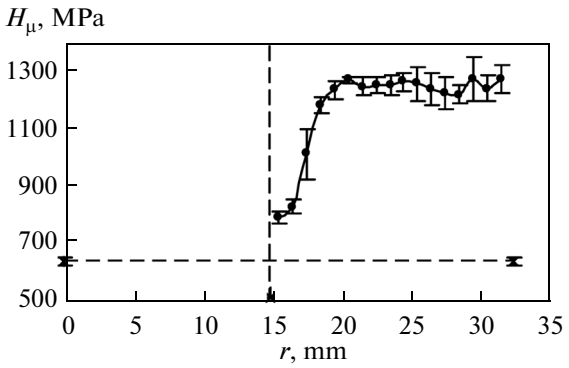

Fig. 7. Variation of the microhardness of the sample along the radial direction. Horizontal dashed line corresponds to the copper microhardness in the initial state; vertical dashed line, to the boundary of the internal cavity.

The microhardness of copper in the initial state is $H_\mu = 626 \pm 16$ MPa. Figure 7 shows the variations in the microhardness of copper after explosive loading depending on the radius r in the unbroken sample. It can be seen from the graph that, after loading, the magnitude of the microhardness in the subsurface and middle layers is on average two times higher than that in the initial state. When approaching the internal cavity, the microhardness decreases, but it does not drop to the values of H_μ characteristic of the initial state. The last two points in the graph correspond to layers containing recrystallized grains. The minimum value of H_μ for the layer located 0.7 mm away from the cavity is equal to 779 MPa, which is 24% higher than the microhardness of copper in the initial state. This is mainly related to the significantly smaller size of the recrystallized grains compared to that in the initial state.

The electron-microscopic investigation reveals a large amount of dislocations in the subsurface layers of the ball. The dislocations are located randomly and no cellular structure is formed (Fig. 8). Along with chaotically distributed dislocations, microbands are present akready in the surface layers in the deformed structure of copper (Figs. 8a, 9a). The formation of microbands upon the shock compression of metals and alloys with an fcc structure was for the first time observed in [16–19]. In [13], it was shown that the propagation of such microbands occurs on {111} planes. The boundaries of the microbands can be both very thin (Figs. 8a, 9a) and strongly smeared (Fig. 9b). However, in both cases, the dislocation density in the boundaries of microbands is very high. Near the bands and inside them, in some cases, a strong deformation contrast is observed that is related to the presence of elastic-stress fields (Fig. 9a).

With increasing the depth of the location of the layer, the amount of microbands increases, and, in some cases, a change occurs in their appearance (Figs. 9b, 9c). This change is apparently related to the beginning of the process of polygonization, which leads to the formation of a banded structure. The onset of the formation of the banded structure is especially clear in Fig. 9c. In some cases, regions can be seen that contain a banded structure that formed as a result of slip on two slip systems (Fig. 10).

In the layer with $r = 24.4$ mm, a small amount of microbands are present, but mainly a banded structure is observed. In some cases, at the boundaries of these bands, small fragments with an alternating black-and-white contrast can be seen, which indicates the occurrence of polygonization processes (Fig. 11a). The presence of the black-and-white contrast upon the formation of low-angle boundaries was observed, e.g., in [20]. It can clearly be seen in the dark-field images that polygonal boundaries are also formed inside the bands (Fig. 11b). Along with polygonization, the formation of fine recrystallized grains also occurs in some regions (Fig. 11c).

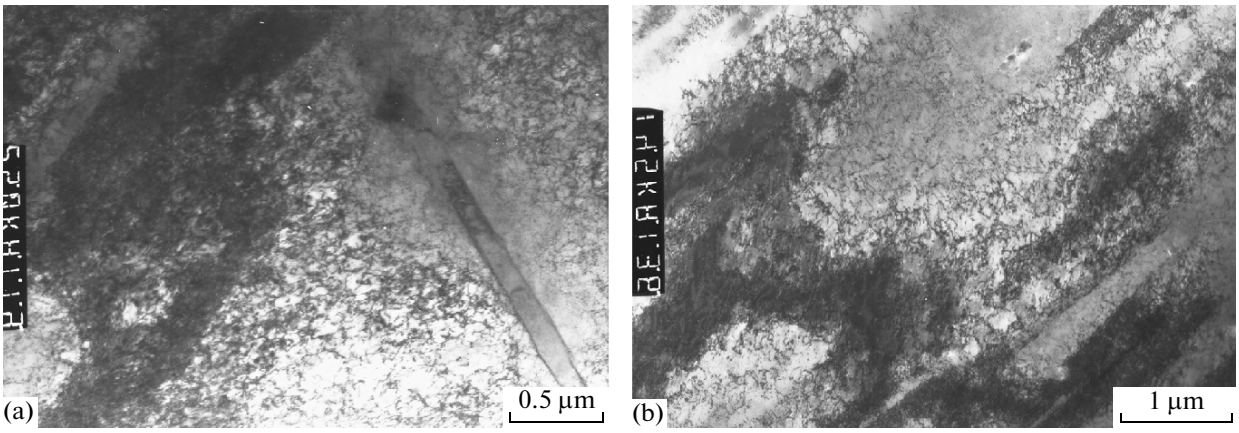

Fig. 8. Dislocation structure of copper in regions located at various r in the retained sample: (a) $r = 31.9$ and (b) 29.4 mm.

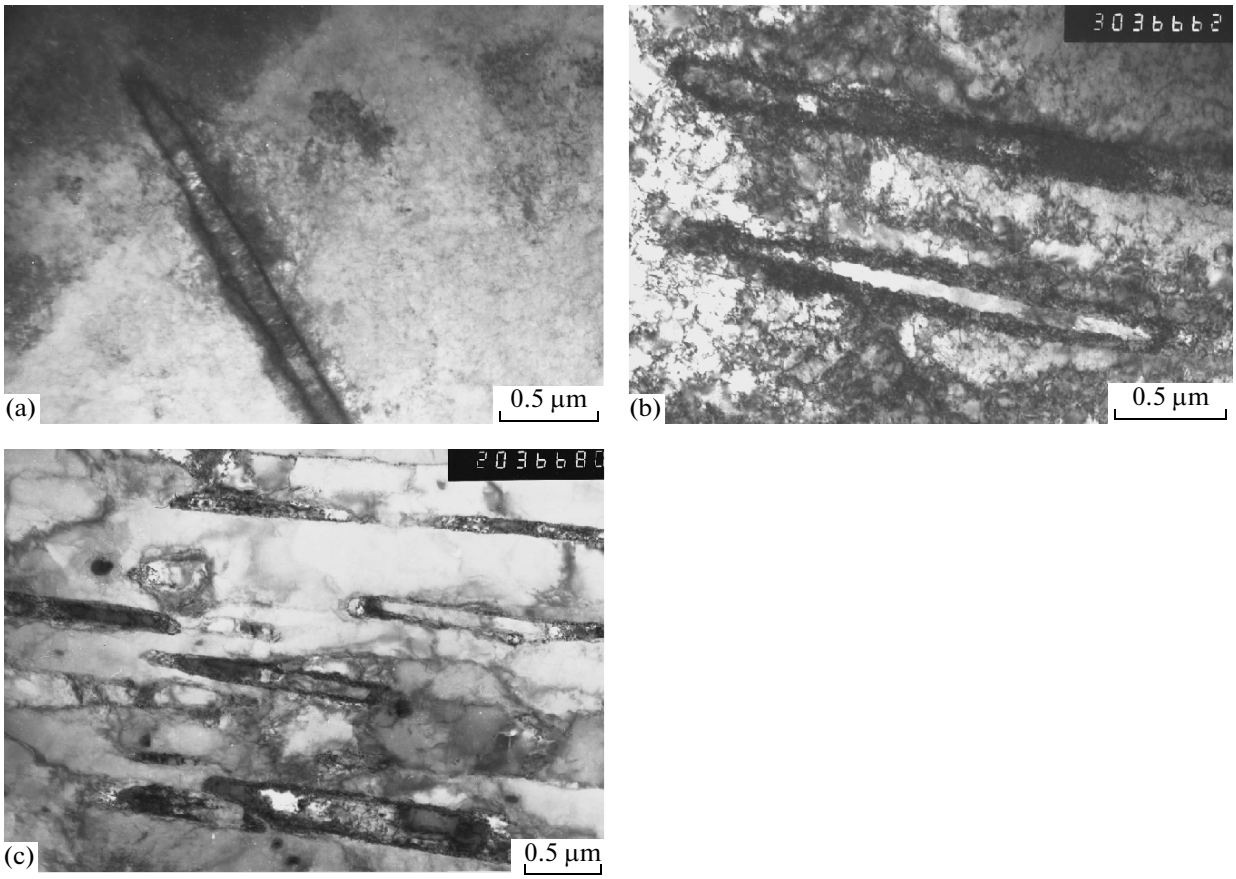

Fig. 9. Microbands in copper in regions located at various r in the retained sample: (a) 31.9 and (b, c) 26.9 mm.

Along with dislocations and microbands, microtwins arise in the structure of the ball after shock loading (Fig. 12). They either are observed as single twins or form pileups. No significant difference is observed in the amounts of microtwins in this ball compared to their number after low-intensity loading regime.

In the deformation structure of the layer located at $r = 21.0$ mm, some regions with a banded structure are present (Fig. 13a) and, in some regions, new recrystallized grains occur, which appear to arise at sites where localized-deformation bands develop or at the boundaries of initial grains (Fig. 13b). Upon going to the layer with $r = 19.4$ mm, the banded structure begins to be destroyed due to the increase in temperature (Fig. 13c), but the microtwins still are observed in this layer (Fig. 13d). In deeper layers of the ball, recrystallization processes begin developing intensely.

A characteristic feature of the deformation structure of copper after this regime of loading is the presence of a large amount of dislocation loops of the vacancy type (Fig. 14). Deformation contrast is observed around these loops in the form of two arcs.

DISCUSSION

It follows from the results obtained that, as in the case of low-intensity regime of loading, the high-velocity plastic deformation of copper upon high-intensity regime of loading occurs mainly via slip. On the microlevel, shear bands of predominantly one orientation are observed. This character of deformation differs substantially from the deformation of copper upon other loading modes, where different slip systems $\{111\}\langle 110\rangle$ can act sequentially. Initially, the active slip system is the one that has the greatest Schmid factor. As a result of the strain hardening of the material due to the action of the primary slip system, another slip system gradually becomes active with a smaller Schmid factor; correspondingly, upon the metallographic investigation, signs of deformation appear that belong to several slip systems $\{111\}\langle 110\rangle$. Upon loading by spherically converging shock waves, shear bands are observed that belong mainly to one system. The occurrence of deformation in only one slip system indicates that the strain hardening under the effect of this system does not lead to a state in which the system with a smaller Schmid factor becomes active. A possible reason for this may be a

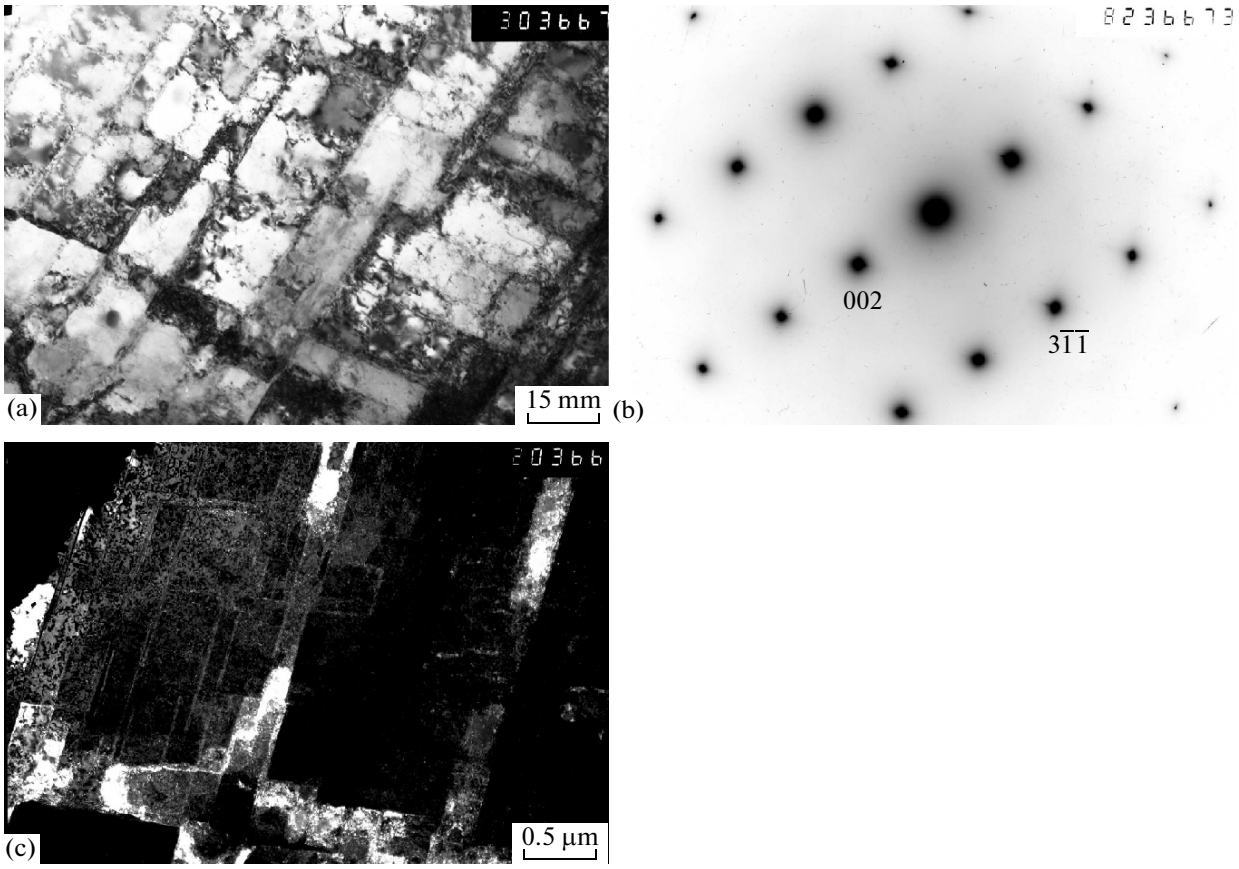

Fig. 10. Banded structure in the layer located at $r = 26.9$ mm formed via slip in two systems: (a) bright-field image; (b) selected-area electron diffraction (SAED) pattern corresponding to (a), zone axis [130]; and (c) dark-field image using reflection (002).

local heating in the slip plane due to adiabatic processes upon the motion of dislocations with high velocities. This leads to a decrease in the flow stress and the localization of deformation via the formation of shear bands. In turn, as follows from the results of [21], a significant increase in temperature occurs in the shear bands. The deformation-induced softening of the material that occurs due to the localization of deformation decreases the probability of passing to other slip systems.

The feature that distinguishes the deformation structure of copper after high-intensity regime of loading from its structure after low-intensity loading is the formation of localized-deformation bands at grain boundaries in deep layers. Due to a temperature increase, fine recrystallized grains are formed inside these bands. Similar bands of localized deformation were observed in our previous works after explosive loading in spherical systems in the deformation structure of artificially aged alloy Al–4 wt % [21], platinum [22], and iron [23, 24].

A characteristic feature of the copper structure on the microlevel is the presence of microbands. In the literature, several classifications of the types of dislocation structures (or substructures) were suggested with different degrees of fineness. The character of the spatial distribution of dislocations and the presence of misorientations of microregions of the crystal relative to each other can serve as the classification signs. The main types of dislocation structures that are observed in metals and alloys at moderate temperatures and strain rates are a chaotic distribution of dislocations, a cellular structure, and a banded structure. The banded structure is formed at the stage of developed plastic deformation. It was also noted that, upon shock loading (at high strain rates), the formation of microbands is observed in the structure. These microbands cannot be classified as classical banded structures, since they are observed at moderate degrees of deformation; nevertheless, in some sense, they can be considered as the initial stage of the formation of a banded structure. In [17, 18], the formation of microbands was ascribed to the occurrence of several sequential processes. At the initial stage, the annihilation of dislocations occurs in the primary slip planes, which leads to the creation of a dislocation-free channel, which is surrounded by double dislocation walls. At the next stage, the activation of secondary slip systems leads to the formation of Lomer–Cottrell barriers, which block slipping. The absence of a cellular structure in our case indicates

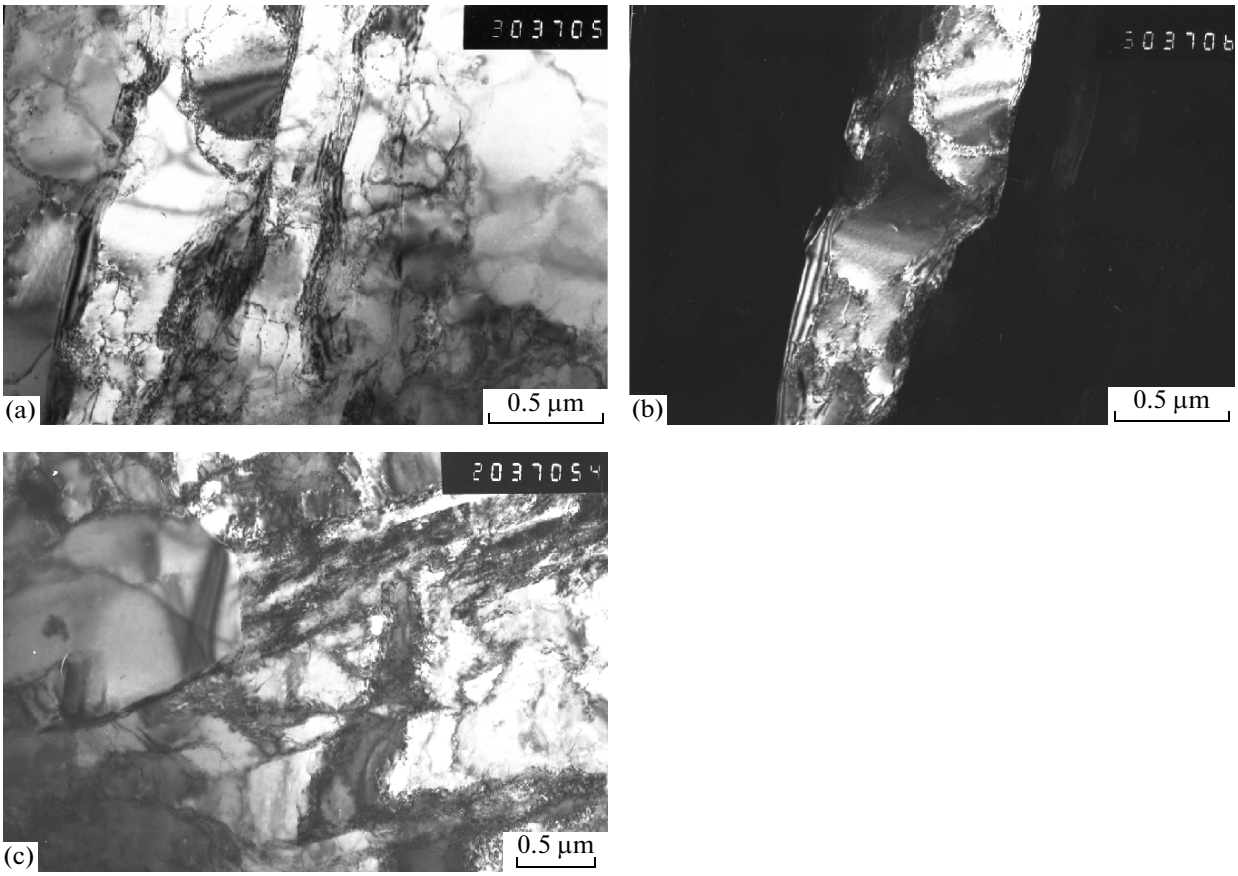

Fig. 11. Banded structure in the layer located at $r = 24.4$ mm: (a, c) bright-field images; (b) dark-field image in the reflection {111} corresponding to (a).

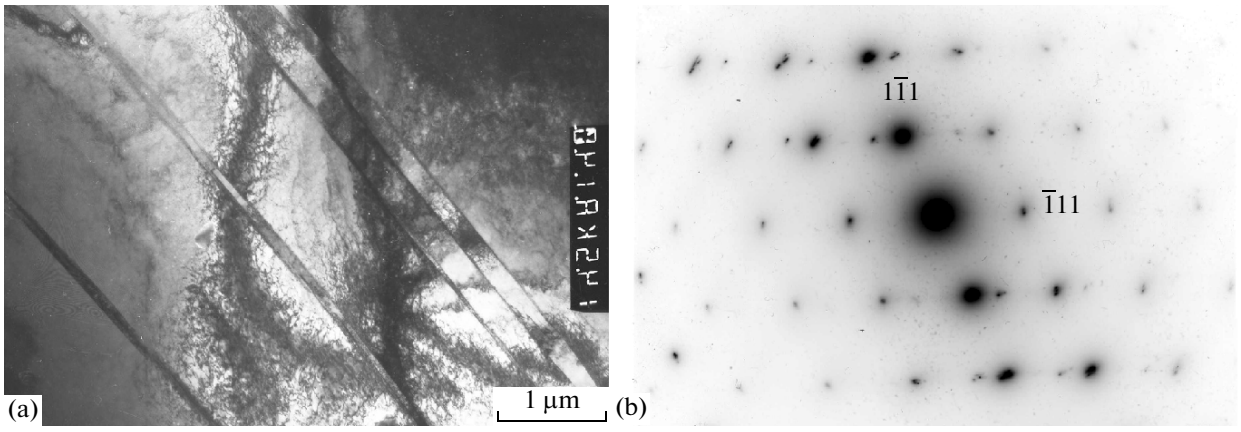

Fig. 12. Microtwins in copper after loading: (a) bright-field image; (b) SAED pattern corresponding to (a), zone axis of the main orientation [110].

that no formation of a significant amount of Lomer–Cottrell barriers occurs. Therefore, it can be supposed that the probable reason for the formation of microbands is the strong localization of deformation at the front of the shock wave because of the inhomogeneity of the material, which leads to the appearance of bands with a high density of dislocations. The localization of deformation is accompanied by the strong heating of the material, which, because of the dissipative processes, leads to the appearance of channels free of dislocations inside the band.

A comparison of the broadening of diffraction lines of polycrystalline copper after high- and low-intensity regimes of loading shows that, within the error of measurements, it remains approximately unaltered. The

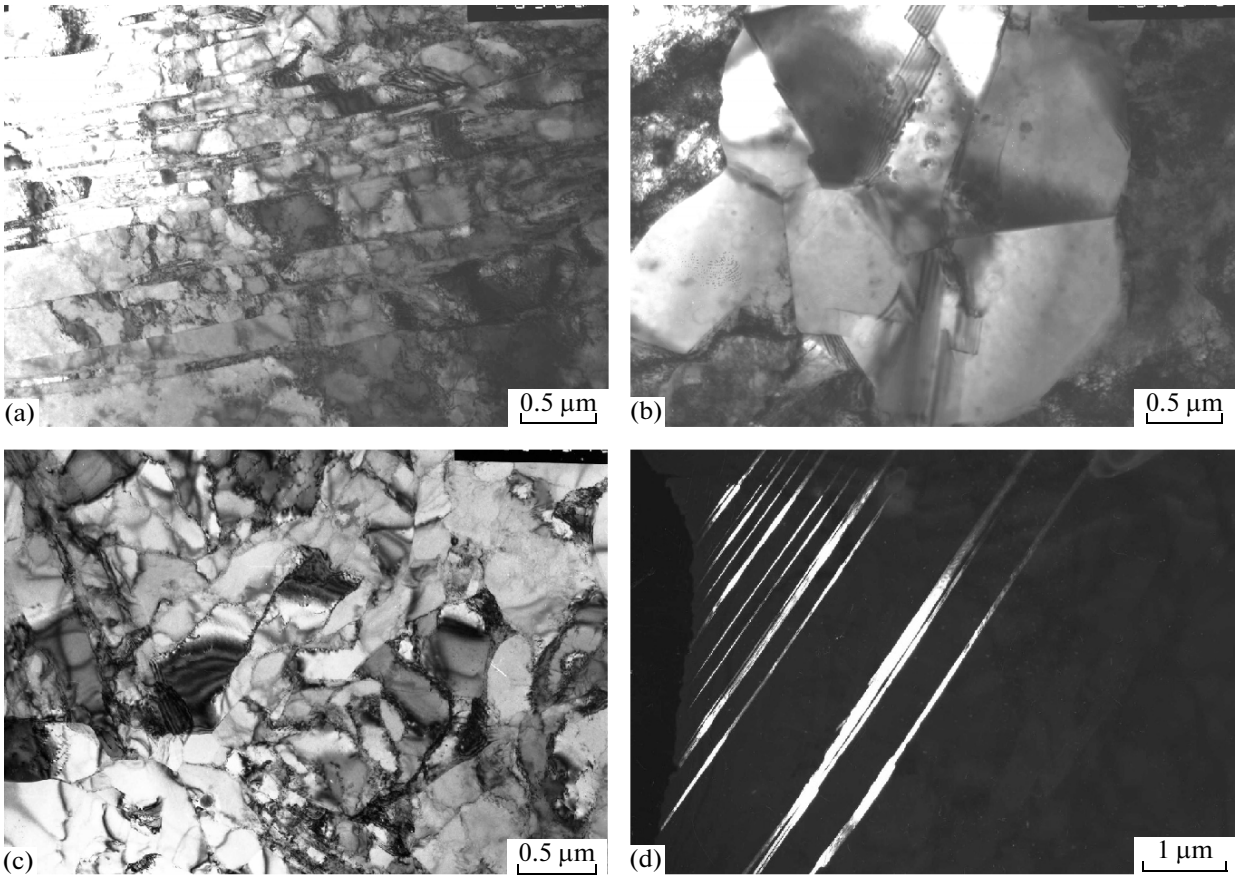

Fig. 13. Deformation structure of copper in the regions located at various values of r in the retained sample: (a, b) $r = 21.9$ mm; (c, d) 19.4 mm; (d) dark-field image in the reflection $(1\,\bar{1}\,1)_{tw}$.

only difference is that, in the case of the low-intensity mode of loading, the half-width of diffraction lines is independent of the depth at which the layer is located in the ball, whereas in the case of the high-intensity regime of loading, the broadening decreases in the layers located at $r = 20.0$ mm and deeper, which is due to the occurrence of processes of recovery and recrystallization. The variations in the broadening of diffraction lines for both regimes of loading correlate with the behavior of microhardness; in both cases, the microhardness of copper increases by about a factor of two and is independent of the layer position in the ball; its decrease in the deeper layers of the ball subjected to high-intensity loading is related only to processes of recovery and recrystallization. Electron-microscopic investigation has shown that, even at the equal broadening of the lines and equal values of the microhardness, the microstructure of the balls can differ substantially; in the case of the high-intensity loading, the copper structure contains a greater amount of microbands and a banded structure is developed in it. The equal broadening of diffraction lines for the different types of dislocation structures indicates that the line broadening reflects only the total microdeformation of the crystal lattice. It can be seen from the data obtained that the magnitude of the pressure at the front of the spherically converging shock wave does not exert a significant effect on the total microdeformation of the crystal lattice.

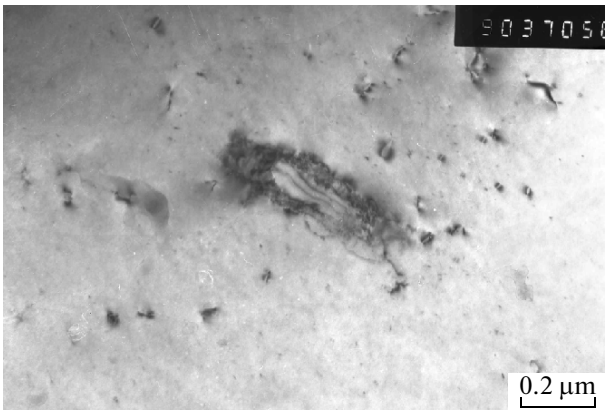

Fig. 14. Vacancy-type dislocation loops in copper after loading.

The authors of [25] performed an X-ray diffraction study of the dislocation density in copper after high-velocity loading by shock and quasi-isentropic waves of different amplitudes. It was established in that work that the dislocation density depends on the loading mode, strain rate, grain size, and magnitude of pressure. Upon the shock-wave loading, the dislocation density increased with increasing pressure, whereas upon the quasi-isentropic wave loading, this density was almost independent of pressure, but increased with increasing deformation rate. Unfortunately, no electron-microscopic study of the dislocation structure was performed in that work; therefore, just as in our work, the broadening of diffraction lines observed by the authors apparently reflected only the total microdeformation of the crystal lattice.

The absence of the dependence of the broadening of XRD lines on the magnitude of pressure upon loading by spherically converging shock waves in this work and by quasi-isentropic waves in [25] and the presence of such a dependence upon the shock wave loading in [25] indicate that the mode of loading exerts a substantial effect on the total microdeformation of the crystal lattice of the material.

A substantial difference of the structure of copper subjected to high-intensity loading is that, with increasing depth of the layer location in the ball, the recrystallization processes begin to occur and a layer of crystallized metal is formed in the layers around the cavity. A quantitative estimation yielded the following values: the volume of the crystallized metal $V_L \approx 290$ mm^3 and, for the mass of the molten copper, $m_L \approx 2.6$ g. According to [26], melting at the shock adiabat occurs at a pressure of 200 GPa and, at the isentrope, upon the decompression from pressures of ~150 GPa. It follows from our data that the melting of copper occurred in layers located at $R \le 4.1$ mm. Based on the calculated data given in Fig. 3, it can be seen that the melting at the isentrope should occur at $R \le 6$ mm. This value is significantly larger than that obtained in experiments. This difference may be due to the fact that the calculated values were obtained based on the assumption that the layer of the explosive was initiated simultaneously over the entire external surface of the ball. Therefore, these values are maximum possible parameters of loading that could be achieved in this experiment.

CONCLUSIONS

In this work, we have studied the effect of spherically converging shock isentropic waves on the deformation behavior of polycrystalline coarse-grained copper subjected to high-intensity loading. It has been shown that, under the loading conditions employed, the main mechanisms of plastic deformation of polycrystalline copper are the slip and deformation localization at grain boundaries. In the process of high-velocity plastic deformation, shear bands arise that mainly belong to one slip system. At the microlevel, a homogeneous dislocation structure, microbands, microtwins, a banded structure, and vacancy dislocation loops have been observed. No cellular structure is formed.

ACKNOWLEDGMENTS

This work was supported in part by the project no 12-P-2-1009 of the Program of Basic Research of the Presidium of the Russian Academy of Sciences "Condensed Matter under the Effect of High Energy Densities."

The electron-microscopic investigation was performed using JEM-200CX and Philips CM 30 electron microscopes at the Center of Collaborative Access of the Institute of Metal Physics, Ural Branch, Russian Academy of Sciences.

REFERENCES

1. J. George, "An electron microscope investigation of explosively loaded copper," Philos. Mag. **15**, 497–506 (1967).
2. M. Mogilevskii, "A structural changes in pure copper subjected to explosive loading," Combust., Explos., Shock Waves **6**, 197–201 (1970).
3. L. E. Murr, "Work hardening and the pressure dependence of dislocations density and arrangements in shock loaded nickel and copper," Scr. Metall. **12**, 201–206 (1978).
4. M. A. Meiers and L. E. Murr, "Defect formation at deformation by shock wave," in *Shock Waves and High-Strain-Rate Phenomena in Metals: Concepts and Applications*, Ed. by M. Meyers and L. E. Murr (Plenum, New York, 1981; Metallurgiya, Moscow, 1984).
5. L. E. Murr, "Microstructure and mechanical properties of metals and alloys after loiading by shock waves," in *Shock Waves and High-Strain-Rate Phenomena in Metals: Concepts and Applications*, Ed. by M. Meyers and L. E. Murr (Plenum, New York, 1981; Metallurgiya, Moscow, 1984).
6. M. A. Mogilevskii and L. S. Bushnev, "Deformation structure development in Al and Cu single crystals on shock-wave loading up to 50 and 100 GPa," Combust., Explos., Shock Waves **26**, 215–220 (1990).
7. P. S. Follansbee and G. T. Gray III, "Dynamic deformation of shock prestrained copper," Mater. Sci. Eng., A **138**, 23–31 (1991).
8. B. Y. Cao, D. H. Lassila, M. S. Schneider, B. K. Kad, C. X. Huang, Y. B. Xu, D. H. Kalantar, B. A. Remington, and M. A. Meyers, "Effect of shock compression method on the defect substructure in monocrystalline copper," Mater. Sci. Eng., A **409**, 270–281 (2005).
9. J. Petit and J. L. Dequiedt, "Constitutive relations for copper under shock wave loading. Twinning activation," Mechan. Mater. **38**, 173–185 (2006).
10. A. V. Dobromyslov, N. I. Taluts, and E. A. Kozlov, "High-rate plastic deformation of a copper single crystal under loading by spherical converging shock waves," Int. J. Mater. Res. **100**, 395–398 (2009).

11. B. Cao, D. H. Lassila, C. Huang, Y. Xu, and M. A. Meyers, "Shock compression of monocrystalline copper: Experiments, characterization, and analysis," Mater. Sci. Eng., A **527**, 424–434 (2010).
12. A. M. Podurets, V. A. Raevskii, V. G. Khanzhin, A. I. Lebedev, O. N. Aprelkov, V. V. Igonin, I. N. Kondrokhina, A. N. Balandina, M. I. Tkachenko, Zh. Zh. Peti, and M. E. Zokher, "Twin structures in copper after shock and shockless high-rate loading," Combust., Explos., Shock Waves **47**, 606–614 (2011).
13. A. V. Dobromyslov, N. I. Taluts, E. A. Kozlov, A. V. Petrovtsev, and D. T. Yusupov, "Deformation behavior of copper upon loading by spherically converging shock waves: Low-intensity loading conditions," Phys. Met. Metallogr. **114**, 358–365 (2013).
14. A. T. Sapozhnikov and A. V. Pershina, "Interpolation equation of state in evaporation area," Vopr. At. Nauki Tekhn., Ser. Metodiki Programs Chisl. Reshen. Zadach Matem. Fiz., No. 2 (16), 29–34 (1984).
15. A. T. Sapozhnikov, P. D. Gershchuk, E. L. Malyshkina, E. E. Mironova, and L. N. Shakhova, "GLOBUS broad range table equation of state and its application for description of thermodynamical properties of copper," Vopr. At. Nauki Tekhn., Ser. Matem. Model. Fiz. Proc., No. 1, 9–17 (1991).
16. G. T. Gray III, "Deformation twinning in Al–4.8% Mg," Acta Metall. **36**, 1745–1754 (1988).
17. J. C. Huang and G. T. Gray III, "Influence of precipitates on the mechanical response and substructure evolution of shock-loaded and quasi-statically deformed Al–Li–Cu alloys," Metall. Mater. Trans. A **20**, 1061–1075 (1989).
18. J. C. Huang and G. T. Cray III, "Microband formation in shock-loaded and quasi statically deformed metal," Acta Metall. **37**, 3335–3347 (1989).
19. J. C. Sanchez, L. E. Murr, and K. P. Staudhammer, "Effect of grain size and pressure on twinning and microbanding in oblique shock loading of copper rods," Acta Mater. **45**, 3223–3235 (1997).
20. P. B. Hirsch, R. W. Horne, and M. J. Whelan, "Direct observations of the arrangement and motion of dislocations in aluminium," Philos. Mag. **1**, 677–684 (1956).
21. A. V. Dobromyslov, N. I. Taluts, E. A. Kozlov, and A. N. Uksusnikov, "Effect of spherically converging shock waves on the phase and structural states of the artificially aged Al–4 wt % Cu alloy," Phys. Met. Metallogr. **113**, 418–425 (2012)
22. E. A. Kozlov, A. V. Dobromyslov, B. V. Litvinov, N. I. Taluts, G. V. Kovalenko, G. G. Bondarchuk, and G. V. Dolgikh, "Deformation behavior of platinum and a Pt–25% Ir alloy under spherical shock waves," Phys. Met. Metallogr. **95**, 200–208 (2003).
23. A. V. Dobromyslov, E. A. Kozlov, and N. I. Taluts, "High-strain-rate deformation of Armco iron induced by spherical and quasi-spherical converging shock waves and the mechanism of the $\alpha \rightarrow \varepsilon$ transformation," Phys. Met. Metallogr. **106**, 531–541 (2008).
24. E. A. Kozlov, A. V. Dobromyslov, N. I. Taluts, and K. Vol'ts, "Effect of spherically converging shock waves on deformation and phase behavior of high-purity iron," Phys. Met. Metallogr. **113**, 1007–1015 (2012).
25. A. M. Podurets, M. I. Tkachenko, O. N. Ignatova, A. I. Lebedev, V. V. Igonin, and V. A. Raevskii, "Dislocation density in copper and tantalum subjected to shock compression depending on loading parameters and original microstructure," Phys. Met. Metallogr. **114**, 440–447 (2013).
26. V. D. Urlin, "Melting at ultrahigh pressures obtained in shock waves," Zh. Eksper. Teor. Fiz. **49**, 485–492 (1965).

Translated by S. Gorin